AD-A042 069 CITY COLL NEW YORK DEPT OF PHYSICS F/G 7/4
KINETIC THEORY DESCRIPTION OF ELECTRON STIMULATED DESORPTION.(U)
JUN 77 R JANOW, N TZOAR N00014-75-C-0949

UNCLASSIFIED NL

| OF |
AD
A042 069

END

DATE
FILMED
8-77

SECURITY CLASSIFICATION OF THIS PAGE (When Data Entered)

REPORT DOCUMENTATION PAGE

READ INSTRUCTIONS BEFORE COMPLETING FORM

1. REPORT NUMBER	2. GOVT ACCESSION NO. 3. RECIPIENT'S CATALOG NUMBER
4. TITLE (and Subtitle) Kinetic Theory Description of Electron-Stimulated Desorption.	5. TYPE OF REPORT & PERIOD COVERED Technical Rept.
	6. PERFORMING ORG. REPORT NUMBER
7. AUTHOR(s) Richard Janow, Narkis Tzoar	8. CONTRACT OR GRANT NUMBER(s) N00014-75-C-0949
9. PERFORMING ORGANIZATION NAME AND ADDRESS Physics Department, City College, New York, N.Y. 10031	10. PROGRAM ELEMENT, PROJECT, TASK AREA & WORK UNIT NUMBERS NR-392-012
11. CONTROLLING OFFICE NAME AND ADDRESS Office of Naval Research (Code 421) Arlington, Virginia 22217	12. REPORT DATE June 30, 1977
	13. NUMBER OF PAGES 36
14. MONITORING AGENCY NAME & ADDRESS (if different from Controlling Office) Office of Naval Research, 715 Broadway, N.Y., N.Y. 10003	15. SECURITY CLASS. (of this report) UNCLASSIFIED
	15a. DECLASSIFICATION/DOWNGRADING SCHEDULE

16. DISTRIBUTION STATEMENT (of this Report)

Approved for public release; distribution unlimited

(11) 30 Jun 77

(12) 37 p.

17. DISTRIBUTION STATEMENT (of the abstract entered in Block 20, if different from Report)

Approved for public release; distribution unlimited

18. SUPPLEMENTARY NOTES

To be published in Surface Science

19. KEY WORDS (Continue on reverse side if necessary and identify by block number)

Electron-Desorption, Angular Dependence, Chemisorption, Tungsten

20. ABSTRACT (Continue on reverse side if necessary and identify by block number)

A first principles kinetic theory is developed, applicable to angular dependent emission in Electron Stimulated Desorption. Expressions for the ionic and neutral atom ESD cross sections are formulated and applied in a model calculation of 0^+ emission from W (111). Strong focussing of the outgoing ions was found, with the use of a model ion-solid potential in which the substrate was free of excitation. Off-axis spot groups were simulated. The peak ion energies obtained with this model are, however, small compared to experimental energies for the high coverage case. The need to to introduce substrate excitations to describe this case is discussed.

DD FORM 1 JAN 73 1473 EDITION OF 1 NOV 65 IS OBSOLETE S/N 0102-014-6601 |

UNCLASSIFIED

SECURITY CLASSIFICATION OF THIS PAGE (When Data Entered)

404 398

(12)

Kinetic Theory Description of Electron Stimulated Desorption

by

Richard Janow and Narkis Tzoar
Department of Physics
The City College of the City University of New York
New York, New York 10031

*Research Sponsored in part by the U.S. Office of Naval Research under ONR contract. No. N00014 - 75 - C - 0949 and in part by the City University Faculty Research Award Program.

ABSTRACT:

A first principles kinetic theory is developed, applicable to angular dependent emission in Electron Stimulated Desorption. Expressions for the ionic and neutral atom ESD cross sections are formulated and applied in a model calculation of O^+ emission from W(111). Strong focussing of the outgoing ions was found, with the use of a model ion-solid potential in which the substrate was free of excitation. Off-axis spot groups were simulated. The peak ion energies obtained with this model are, however, small compared to experimental energies for the high coverage case. The need to introduce substrate excitations to describe this case is discussed.

I. INTRODUCTION

Much work has been done in recent years on the phenomenon of Electron Stimulated Desorption (ESD). In these experiments, a beam of low energy electrons, in the range of 100-500 ev impinges on an adsorbate covered surface, causing the ejection of ions or neutral particles. Several articles reviewing ESD have appeared.[1 - 4]

Experimental data have been collected about the ion yields and cross sections. Energy distributions of emerging ions have been measured.[5] In the last several years, the angular distribution of ejected ions has been investigated.[6-8] Strong focussing of the desorbing ions has been revealed. Desorption patterns were obtained which contain sets of well defined cones for ion emission, both normal and non-normal to the surface. The number and orientation of emission cones is related to the substrate geometry.

ESD Ion Angular Distributions may thus provide valuable clues to the adsorption geometry, on the scale of the unit cell size. This direct information is complementary to that obtained , for example, by LEED, which is sensitive to mainly long range order in the adsorbed layer and substrate.

In this theoretical work, we address ourselves primarily to the angular dependence problem. Previous theoretical treatments of ESD have been strictly one dimensional, and phenomenological in flavor.[9,10] This work presents a first principles transport formulation of the desorbing ion dynamics. The ion -solid interactions are assumed to be time independent, or long lived relative to ion flight times.

Section II establishes the conceptual framework and introduces kinetic equations which can be solved formally, in three dimensions, for the linear response to external electron bombardment. In Section III, expressions for the ionic and neutral atom ESD cross sections are obtained from the kinetic theory, in a form suitable to efficient numerical integration. Section IV is an illustrative model calculation of ESD Ion Angular Distributions. The experimentally interesting case of O^+ desorption from W (111) was chosen, with the surface assumed free of excitation during the ion ejection. Section V is reserved for discussion.

We found that ion interactions with a ground state surface can replicate the focussing and ion distributions in experimental ESD patterns, for several adsorption geometries. However, this model surface potential probably cannot explain the large O^+ ion energies observed at high coverage. We speculatively suggest that long lived excitations on the surface may play the dominent role in ESD of O^+ at high coverage.

II. FORMULATION OF THE PROBLEM

This calculation employs a multi-step picture of the desorption process which has been found useful in previous ESD investigations.[1-4,9-11] Adsorbed particles are Franck-Condon excited to an anti-bonding state from which ionic desorption may occur. Propagation follows, with the dynamics determined by an effective adparticle-surface interaction potential. Recapture may occur via bond healing transitions. Reneutralized particles may still possess sufficient kinetic energy to escape as neutrals, in which case ground state propagation completes the desorption process.

The above picture is useful for describing the response of adparticle substrate systems which are interacting weakly with an external beam. Hence, we linearize the kinetic equations presented below in the incident flux. Adparticle propagation is described classically. The excitation and decay mechanisms involve electronic transitions, and thus require quantum mechanical descriptions.

A single atom or molecule interacting with a surface may be described by the following Hamiltonian:

$$H = -\frac{\nabla_r^2}{2M} + H_e(\vec{r}, \vec{r}_i) \qquad (1)$$

Here, H_e contains all the potentials in the system, as well as kinetic energy operators for electrons which participate in atom-surface interactions. The kinetic energy operator shown acts on adparticle mass center coordinates, with M denoting the adparticle mass.

In the Born-Oppenheimer Approximation, the propagation phase of desorption decouples, to order m_e/M, from the electronic states of the system. Electronic responses to shifts in the adparticle coordinates may be regarded as instantaneous, permitting a set of effective interaction potentials to be defined.

Excitation and reneutralization are likewise regarded as sudden, inelastic events in which the internal adparticle state, and thus the propagation dynamics, change discontinuously. We assume that the asymptotically recognizable adparticle states partially diagonalize H_e close to the surface.

For the present, consideration is restricted to a two level system, with n=1 for the neutral ground state. For positive ions, n=2. The z-dependent behavior of the effective potentials $E_n(\vec{r})$ is sketched qualitatively in Fig. 1. The minimum of $E_1(\vec{r})$ lies at the chemisorption site. In order for ionic desorption to occur, the antibonding curve $E_2(\vec{r})$ must have the generally repulsive character shown. One expects E_2 to become attractive at long range due to image charge density residing on the surface. The difference $[E_2(\vec{r}) - E_1(\vec{r})]$ is regarded as the internal ionization energy of the adsorbate. At large adsorbate to surface separations it is identical to the free atomic value. Variations of $E_n(\vec{r})$ in the plane parallel to the surface are crucial for the angular dependent desorption problem, and are discussed below.

This picture of desorption, and the transport theory developed below, may be readily generalized to include multiple excited state systems, in which substrate excitations and neutral excited states of adparticles must be considered. In addition, photodesorption may be treated within basically the same formalism.[12]

Little attention in the literature has been given to the ionic states which govern the desorption kinetics. Most work has focussed on the ground state potential minima, where adsorption occurs. Studies of electron dissociation of molecules furnish a guide to the antibonding states, however, the model adopted for E_2 in this preliminary study is likely to be crude. The difficulties involved in modelling E_2 for positively ionized cores, are less formidable than for neutrals or negative ions, for which exchange and correlation effects may be important.

The functions $E_n(\vec{r})$ are assumed known in developing a kinetic theory below. Furthermore, the solutions of the classical equations of motion for ions and neutral particles are assumed to be known, and to adequately describe propagation of the massive adparticles. The classical solutions $\vec{r}_n(t)$ depend parametrically on time and on the initial coordinates for each adparticle trajectory.

This classical description is most applicable to unbound, and hence desorbing states. Ions in state 2 quickly acquire substantial kinetic energy. The same argument applies to atoms desorbing in the ground state after suffering reneutralization. A classical description is also acceptable for vibrational states of massive adatoms at high temperatures, that is, when $\hbar\omega_o \ll kT$. Here, $\hbar\omega_o$ may be taken to be the level spacing for a harmonic oscillator approximation to E_1 near the chemisorption site.

When $\hbar\omega_o \geq kT$, classical kinetic equations still provide qualitatively correct results for the linear response. The propagation of particles only in unbound trajectories need be followed. The principal correction introduced by quantizing the vibrational states is to modify the shape of ion energy distributions.

We denote by $R(\vec{r})$, $Q(\vec{r})$ the transition rates for ionization and reneutralization respectively. These functions, assumed known, of adatom-coordinate $\vec{r}$ are averaged over all initial and final states of the substrate and incident electron consistent with a change of adatom state. Inasmuch as the dominant impulse to adsorbed or desorbing particles is provided in this picture by the gradients of E_n, the small recoil suffered during ionization or non-radiative decay will be neglected.

Electronic energies generally employed in ESD experiments lie in the range 100 - 500 ev. So long as incident electrons are of high but non-relativistic

energy, the excitation phase of ESD may be described in the Born Approximation. For simple ionization processes, the coordinates of two final state electrons are averaged over in $R(\vec{r})$. These exit quickly from the surface region, and are either absorbed by the solid or emitted as Auger electrons to the vacuum. Inasmuch as incident electron energies are large compared to $(E_2 - E_1)$, ionization can occur from within the entire Franck-Condon region.

Non-radiative decay channels dominate transitions back to the ground or low lying excited states. Optical decays are discounted, as their lifetimes are long compared to typical ionic flight times. Ion reneutralization involves matrix elements for electron capture from the solid. Hence, this process is efficient at close range, and weakens rapidly with increasing distance from the surface.

The surface plane is assumed to be tessellated by a periodic grid of surface unit cells, each of which is anisotropic in the x-y direction. We regard this structure as known. ting of the surface, or rearrangements of the substrate layer spacing ch are known to occur under certain conditions, can be incorporated into later calculations as required.

The symmetry and periodicity of the surface mesh are imposed on the functions E_n, R, Q which describe the stages of desorption. Transverse anisotropies in the adparticle-surface interactions become neglible while the atom to surface separation is small compared to the sample dimensions.

We formulate a classical transport theory entirely within a single surface unit cell, extended in the z direction normal to the surface. At macroscopic distances, each such cell behaves as a point source of angular dependent intensity. Transport equations linear in the excitation rate $R(\vec{r})$ are now obtained. The rate $Q(\vec{r})$ is treated as a zero order quantity. Later calculations verify that the desorption cross sections depend exponentially on $Q(\vec{r})$.

Let $P_n(\vec{r},\vec{v},t)d^3r\,d^3v$ be the probability of finding an atom or ion in state n at time t, within the phase space volume element at $\vec{r}$, $\vec{v}$, where these are the ionic position and velocity. The following normalization is assumed, for the present:

$$\sum_{n=1,2}\int_{\text{UNIT CELL}} d^3r\, d^3v\, P_n(\vec{r},\vec{v},t) = 1$$

This condition is relaxed after linearizing the theory.

All spontaneous desorption processes are neglected for the systems we consider at the experimentally interesting temperatures. Thermal desorption may occur as a by-product of local surface heating by the incident electron beam. This effect may be disregarded for weak fluxes.

In the absence of external perturbation, the atom-surface system is taken to be a gas of non-interacting particles in thermal equilibrium with the solid. State 2 is unpopulated, hence:

$$P_2^0(\vec{r},\vec{v}) \approx 0$$

Henceforth, zero superscripts denote equilibrium state quantities. The Boltzmann equation which describes the ground state is:

$$\vec{v}\cdot\vec{\nabla}_r P_1^0 - \frac{1}{M}\vec{\nabla}_r E_1\cdot\vec{\nabla}_v P_1^0 = \left(\frac{dP_1}{dt}\right)_{SURF} \approx 0 \qquad (2)$$

Here, M is the adsorbate mass. The surface interaction term describes collisions between adsorbate atoms and substrate excitations. In the present case, these provide principally a relaxation mechanism for the ground state.

Now we allow the system to be driven off equilibrium by an external electron beam. Competition between the relevent transition mechanisms is summarized in the following kinetic equations:

$$\frac{\partial P_2}{\partial t} + \vec{v}\cdot\vec{\nabla}_r P_2 - \frac{1}{M}\vec{\nabla}_r E_2\cdot\vec{\nabla}_v P_2 = \left(\frac{dP_2}{dt}\right)_E + \left(\frac{dP_2}{dt}\right)_Q$$

$$\frac{\partial P_1}{\partial t} + \vec{V} \circ \vec{\nabla}_r P_1 - \frac{1}{M} \vec{\nabla}_r E_1 \circ \vec{\nabla}_v P_1 = \left(\frac{dP_1}{dt}\right)_{SURF} + \left(\frac{dP_1}{dt}\right)_E + \left(\frac{dP_1}{dt}\right)_Q$$

Here, the subscripts Q, E refer to the quenching, excitation mechanisms. We made the choice $(dP_2/dt)_{surf} \approx 0$, in writing the above, thus neglecting scattering and energy loss of the desorbing ions due to interaction with substrate excitations. Such processes will be studied in future investigations.

Ions entering state 2 are described by the source term $(dP_2/dt)_E$. Inasmuch as recoil is neglected, one may approximate:

$$\left(\frac{dP_2}{dt}\right)_E \approx P_1(\vec{r}, \vec{v}, t) R(\vec{r})$$

The corresponding ground state depletion occuring via the ionization process given by:

$$\left(\frac{dP_1}{dt}\right)_E = -P_1(\vec{r}, \vec{v}, t) R(\vec{r}) \approx -\left(\frac{dP_2}{dt}\right)_E$$

Depletion of the ionic state through reneutralization is given by:

$$\left(\frac{dP_2}{dt}\right)_Q = -P_2(\vec{r}, \vec{v}, t) Q(\vec{r})$$

Reneutralized adparticles, which re-enter the ground state are the only ones which can desorb in state 1. These contribute a distinctly non-thermal component to P_1, which must be proportional to the following repopulation term, neglecting the recoil upon quenching:

$$\left(\frac{dP_1}{dt}\right)_Q \approx P_2(\vec{r}, \vec{v}, t) Q(\vec{r}) \approx -\left(\frac{dP_2}{dt}\right)_Q$$

The following set of kinetic equations, linear in R, describes the angular dependent ESD problem for the weakly perturbed case:

$$\frac{\partial P_2'}{\partial t} + \vec{V}_0 \vec{\nabla}_r P_2' - \frac{1}{M} \vec{\nabla}_r E_2 \circ \vec{\nabla}_v P_2' = P_1^0 R - P_2' Q \qquad (3a)$$

$$\frac{\partial P_1'}{\partial t} + \vec{V}_0 \vec{\nabla}_r P_1' - \frac{1}{M} \vec{\nabla}_r E_1 \circ \vec{\nabla}_v P_1' = P_2' Q \qquad (3b)$$

All terms here are of order R^1, as required. One dimensional analogs of Eqns. (3a, 3b) were employed in previous work on photodesorption.

In obtaining the result above, we recalled that $P_2^0 \approx 0$. Hence, to lowest order $P_2 \approx P_2' \propto R$. The ground state distribution was taken to be:

$$P_1 = P_1^D + P_1^1$$

where the depleted equilibrium component P_1^D is defined to satisfy:

$$\frac{\partial P_1^D}{\partial t} + \vec{V}_0 \vec{\nabla}_r P_1^D - \frac{1}{M} \vec{\nabla}_r E_1 \circ \vec{\nabla}_v P_1^D = \left(\frac{dP_1}{dt}\right)_{SURF} - P_1 R$$

The remaining contribution, P_1^1, is then the solution to Eqn. (3b). Inasmuch as P_1^D satisfies an equation independent of Q, a complete description of ground state desorption is yielded by P_1^1. Eq.(2)was used to approximate $P_1^D \approx P_1^0$ to dominent order in R. For weak coupling to the electron flux, the characteristic survival time in the ground state against ionization is long compared to the time for substrate induced relaxation. The following condition then holds:

$$\left(\frac{dP_1}{dt}\right)_{SURF} >> \left(\frac{dP_1}{dt}\right)_E$$

Depletion of P_1^0 may then be neglected, as its effect on P_2^1 and P_1^1 is of order R^2 at least.

In experimental situations, one ideally observes the current of ions or neutral atoms ejected in each state. Linearity of ESD ion currents with the incident electron flux has been supported by observation. Hence, the intermediate and strong coupling limits of this theory appear to be of little practical interest at present.

III. DESORPTION CROSS SECTIONS

The total cross section for desorption in the n th state is given by:

$$\sigma_n = I_n(L,t) / F\Theta(t)$$

Here, $I_n(z,t)$ is the net adparticle current in state n crossing a plane parallel to the surface at z, at time t, per unit cell. I_n is evaluated for L large compared to unit cell dimensions. I_n is proportional to both the electron flux F, and to $\Theta(t)$, the number of adsorbed atoms per unit cell remaining on the surface at t. The cross sections are independent of F for linear response. The coverage $\Theta(t)$ and current $I_n(L,t)$ have the same time dependence via $e^{-F\sigma t}$; hence, σ_n is time independent as well. Here σ is the desorption cross section summed over all channels, while t is the elapsed time.

For angular dependent ESD studies, the differential desorption currents $I_n(\theta, \omega, t)$, and the differential cross sections $\sigma_n(\Theta,\Phi)$ are of interest. Here Θ,Φ specify the asymptotic emission directions. The asymptotic speeds are integrated over. The total and differential cross sections are related by:

$$\sigma_n = \int d\Omega\, \sigma_n(\Theta,\Phi)$$

One may find explicit expressions for $\sigma_n(\Theta,\Phi)$ in terms of the distribution functions by straightforwardly following the microscopic adparticle flux within one unit cell:

$$\sigma_n(\Theta,\Phi) = \frac{1}{F}\int_0^\infty dv\, v^3 \int_{A_c} d^2\vec{r}_{\parallel}\, P_n(\vec{r}_{\parallel}, z=L, \vec{v})$$

Here $\vec{r}_{\parallel}$ lies in the plane parallel to the surface. A_c is the unit cell area. One first evaluates the current density contribution from $d^3\vec{v}$:

$$\vec{J}_n(\vec{r},\vec{v},t)\, d^3\vec{v} = \Theta(t)\, P_n(\vec{r},\vec{v})\, \vec{v}\, d^3\vec{v}$$

associated with the phase point $\vec{r},\vec{v}$.

In view of the complexities associated with the angular dependence problem, we adopt an approach well suited to numerical simulation of ESD Ion Angular Distributions. The explicit result above for the differential cross sections is cumbersome to implement efficiently on the computer.

The steady state ESD response is found by solving an equivalent time dependent problem. We simulate the flux of ions or neutral atoms desorbed in response to an incident electron pulse of short duration τ, then take the limit $\tau \to 0$. Suitable expressions for the total desorption cross sections are constructed using the transport formulation. Numerical differentiation in the asymptotic plane allows one to recover the angular dependence.

This strategy is implemented using the time ordered picture of ESD. An ensemble of adsorbed ground state atoms is perturbed at t = 0 by the electron beam. The forward evolution of the system is followed, without further interaction with the external beam, to a time t, when all ions or reneutralized atoms which can desorb have crossed a detection plane. Each trajectory must be individually followed to its asymptotic direction via the classical equations of motion. One evaluates the contribution made by each ion or atom to the cross section, including attenuation due to quenching.

Time dependent solutions of the kinetic equations are required. The formal solutions for P_n map the evolution of an initial distribution function forward in time. These are used to construct the desorption cross sections.

By convention, the dependence of all quantities on $\vec{r}, v$, is suppressed, with only their parametric time dependence displayed. The classical dynamics problem will be solved numerically. Liouvilles Theorem prompts the replacement in Eqns (3a,3b):

$$\frac{\partial}{\partial t} + \vec{V} \circ \vec{\nabla}_r + \vec{a} \circ \vec{\nabla}_v \longrightarrow \frac{d}{dt}$$

Here, a is the acceleration in the n th state given by:

$$\vec{a} = -\frac{1}{M} \nabla_{\vec{r}} E_n(\vec{r})$$

Equations (3a,3b) now take the form:

$$\frac{d P_2'(t)}{dt} = P_1^0(t) R(t) - P_2'(t) Q(t) \qquad (4a)$$

$$\frac{d P_1'}{dt} = P_2'(t) Q(t) \qquad (4b)$$

First, the ionic survival probability against reneutralization, $S_2(t_o, t)$, is defined to be:

$$S_2(t_o, t) \equiv \exp\left[-\int_{t_o}^{t} dt' Q(t')\right] \qquad (5)$$

The exponent is the reneutralization rate integrated along the ionic trajectory from $\vec{r}(t_o)$ to $\vec{r}(t)$, which is governed by $E_2(\vec{r})$. An alternative notation which displays the path integration explicitly is:

$$S_2(\vec{r}_o, \vec{r}) = \exp\left[-\int_{\vec{r}_o}^{\vec{r}} \frac{Q(\vec{r}') \vec{V}(\vec{r}')}{|\vec{V}(\vec{r}')|^2} \circ d\vec{r}'\right.$$

Here, $\vec{v}(\vec{r}')$ is the ionic velocity at $\vec{r}'$.

It is useful to interpret $S_2(t_o, t)$ as an evolution operator, which maps ions from their initial to final coordinates. One obtains the form of Eq. (5) by solving Eq. (4a) with the ionization term neglected.

ESD cross sections are experimentally found to be several orders of magnitude smaller than atomic or molecular ionization cross sections would indicate. Hence, quenching is presumed to be efficient and we expect $S_2(t_o, t) \ll 1$, when $\vec{r}(t_o)$ is close to the surface, and $\vec{r}(t)$ lies in the detection plane. It is also clear that $S_2(t_o, t) \cdot S_2(t, t') = S_2(t_o, t')$, and $S_2(t_o, t) = S_2^{-1}(t, t_o)$.

The following trial solution for $P_2^1(t)$ is adopted:

$$P_2^1(t) = g(t)\, S_2(t_o, t)$$

After formally differentiating the above and comparing with Eq. (4a) the unknown function g(t) is found to satisfy:

$$\frac{dg(t')}{dt'} = R(t')\, P_1^o(t')\, S_2^{-1}(t_o, t')$$

The formal solution $P_2^1(t)$ for the ionic state is

$$P_2'(t) = P_2'(t_o) S_2(t_o, t) + P_1^o(t_o) \int_{t_o}^{t} dt'\, R(t') S_2(t', t) \qquad (6a)$$

Here, we integrated the equation for g(t) formally over $t_o \le t' \le t$. The boundary condition $g(t_o) = P_2^1(t_o)$ is found by taking the limit $t \to t_o + \epsilon$ One notes that $\lim_{t \to t_o} S_2(t_o, t) = 1$. Both R(t), Q(t) are assumed to be mathematically well behaved. The equilibrium distribution satisfied $P_1^o(t) = P_1^o(t_o)$.

The solution $P_2^1(t)$ yields the ionic distribution function which has evolved from the initial distributions $P_2^1(t_o)$ and $P_1^o(t_o)$. The first term in eq. (6a) attenuates the initial ion density, while the second incorporates ionizations which occur during the interval $[t_o, t]$.

The formal solution of Eq. (4a), containing the ground state component of quenched particles, is:

$$P_1'(t) = P_1'(t_0) + \int_{t_0}^{t} dt' P_2'(t') Q(t') \tag{6b}$$

Here, one uses the state 1 dynamics to map $\vec{r}(t)$, $\vec{v}(t')$ forward to time t in the second term.

We construct the cross sections after first examining the response of a single ground state adatom to ionizing transitions during the short finite interval $[-\tau, 0]$. Let $U^+(-\tau, 0)$ be the probability of finding the atom as an ion at t=0. Using Eq. (6a) this is found to be:

$$U^+(-\tau, 0) = \int_{-\tau}^{0} dt' R(t') S_2(t', 0) \tag{7}$$

Here, the choice $P_2^1(-\tau) = 0$ was made, inasmuch as the initial ionic population must be excluded from the response during $[-\tau, 0]$. We normalized to unit source strength with the choice $P_1^0(t_0) = 1$. The explicit value of U^+ is fixed by the choice of initial conditions $\vec{r}(-\tau)$, $\vec{v}(-\tau)$,

Next, a single ion is permitted to evolve from t = 0 to time t, when its velocity has reached the asymptotic value. No further interaction with the external electrons is included hence, we choose $P_1^0(t_0=0) = 0$, and $P_2^1(t_0 = 0) = 1$ in Eqn. (6a, 6b) Conditional probabilities for finding the atom with r(t), v (t) are given by:

$$V^+(0, t) = S_2(0, t)$$

for the ionic state, and

$$V^{o}(0,t) = \int_{0}^{t} dt' S_2(0,t') Q(t')$$

for the ground state. An ion may reneutralize at any time after t= o. Hence, $V^{o}(0,t)$ contains an integration over intermediate times.

The single atom ejection probabilities, $T^{+,o}(-\tau,0,t)$, for the ionic and neutral state, follow the history of an adsorbed atom which responds to the external beam over $[-\tau,0]$

$$T^{+}(-\tau,0,t) = U^{+}(-\tau,0)V^{+}(0,t)$$

$$T^{o}(-\tau,0,t) = U^{+}(-\tau,0)V^{o}(0,t) \qquad (8)$$

These quantities are closely related to the ionic and neutral atom desorption cross sections to be presented below.

Let $\chi_{\epsilon}(\vec{r}_o)$ denote the ionization cross section for an adsorbed atom at the point $\vec{r}_o = \vec{r}(t=0)$. This function must have the free atomic or molecular ionization cross section as its limit when $z_o \to \infty$. Here, ϵ is the incident electron energy. We expect $\chi_{\epsilon}(\vec{r}_o)$ to be linear in the upward transition rate R_{ϵ} as follows:

$$\chi_{\epsilon}(\vec{r}_o) = R_{\epsilon}(\vec{r}_o)/F \qquad (9)$$

Here, F is the incident electron flux.

This result is recovered after first noting that $U^{+}(-\tau,0)/\tau$ is the average ionization rate per atom. The corresponding average ionization cross section per atom is given by:

$$\bar{\chi}_{\epsilon}(-\tau,0) = \frac{1}{F\tau}\int_{-\tau}^{0} dt' R_{\epsilon}(t') S_2(t',0)$$

In the limit $\tau \to 0^+$ one obtains the instantaneous response. R (t') is smoothly varying for ESD, inasmuch as the summations over final state electron coordinates contained in R consume any delta function resonances. One factors $R_\epsilon(t' = 0)$ from the integration above, and makes the replacement $S_2\ (t', 0) \approx S_2\ (-\eta, 0) = 1$ to obtain Eq. (9)

The cross section for the entire process resulting in ionic desorption of an atom initially in the ground state is given by:

$$\sigma_{EJ}^{+}(0,t) = \chi_\epsilon(\vec{r}_0) V^{+}(0,t)$$
$$= \frac{R_\epsilon(\vec{r}_0)}{F}\, \Theta\left(\tfrac{1}{2}MV_0^2 + E_2(\vec{r}_0) - E_2(\infty)\right) \exp\left[-\int_0^t dt' Q(t')\right]$$

Here, the dependence on R and Q is displayed. The step function was inserted to ensure that desorption is energetically possible. One integrates the decay probability appearing in the exponent from point to point as the trajectory is followed. The asymptotic velocity generated by σ_{EJ}^{+} depends on the choice of $\vec{r}_0, \vec{v}_0$. One chooses t for each ion path so that z(t) lies far from the surface.

The analogous ground state ejection cross section is given by:

$$\sigma_{EJ}^{0}(0,t) = \chi_\epsilon(\vec{r}_0) V^{0}(0,t)$$
$$= \chi_\epsilon(\vec{r}_0) \int_0^t dt' Q(t') \exp\left[-\int_0^{t'} dt'' Q(t'')\right] \cdot$$
$$\cdot \Theta\left(\tfrac{1}{2}MV_0^2 + E_2(\vec{r}_0) - E_2(\vec{r}') + E_1(\vec{r}') - E_1(\infty)\right)$$

Here, the step function was evaluated at the reneutralization point, eliminating trapped particles. E_2 governs the path integrations during $[0, t']$, while E_1 determines the dynamics during $[t', t]$. Numerical evaluation of σ_{EJ}^{0}

is expected to be time consuming due to the integration on intermediate times.

Finally, the ensemble averages of ejection cross sections over the phase space coordinates is taken at t=0. The formal solutions which yield the total ionic and neutral atom ESD cross sections are:

$$\sigma_\epsilon^{+} = \int d^3\vec{r}_0\, d^3\vec{v}_0\, P_1^{o}(\vec{r}_0,\vec{v}_0)\, \chi_\epsilon(\vec{r}_0)\, S_2(0,t)\, \Theta\left(\tfrac{1}{2}MV_0^2 + E_2(\vec{r}_0) - E_2(\infty)\right) \tag{10a}$$

$$\sigma_\epsilon^{o} = \int d^3\vec{r}_0\, d^3\vec{v}_0\, P_1^{o}(\vec{r}_0,\vec{v}_0)\, \chi_\epsilon(\vec{r}_0) \int_0^t dt'\, S_2(0,t')\, Q(t') \cdot$$

$$\cdot\, \Theta\left(\tfrac{1}{2}MV_0^2 + E_2(\vec{r}_0) - E_2(\vec{r}') + E_1(\vec{r}') - E_1(\infty)\right) \tag{10b}$$

The equilibrium distribution P_1^{o} was used in averaging, rather than P_1, inasmuch as the ejection cross sections are already linear in R. Eq. (10a) for σ^+ is employed below in the numerical simulation of ESDIAD for O^+ adsorbed on Tungsten.

Note that Eqn (10a) for σ^+ is a generalization of phenomenological expressions which have appeared in the literature. Our previous work on one dimensional Photodesorption theory produced expressions analogous to Eqns(10a,10b) for the optically fluorescent and ground state cross sections.

The result expressed in Eqns (10a), (10b) is model independent, except for general restrictions on R,Q,E_n, and P_1^{o} outlined above. One may use Eqns(10 a,b)in conjunction with model surface interactions to obtain ESDIAD patterns and energy spectra within the Menzel-Gomer, Redhead ESD picture.

Finally, note that the transport approach is applicable to a wide variety of surface phenomena involving propagation of atoms, ions or molecules. In particular, the cross section contributions due to higher order excitation processes in ESD may be obtained without difficulty.

IV MODEL CALCULATION FOR O^+ DESORPTION FROM TUNGSTEN

The remainder of this paper applies the first principles kinetic theory in a model calculation of desorption from tungsten. We attempt to understand the interesting angular and energy dependent ESD results found recently on W (111)[6] by numerically simulating the ESD patterns and ion energy spectra to be expected for atoms adsorbed at various sites on the surface. Little is known of the nature of possible antibonding states for ions; therefore, simple models are adopted for ion-solid and atom-solid interactions. Absolute cross sections were not calculated due to lack of information about wave functions on surfaces. We concentrate on the spectroscopy of ESD; that is, in this paper we have studied only the polar and azimuthal angular dependence and the energy spectra of emerging ions.

Experimentally, a rich diversity of ESDIAD patterns were found on W (111) and W (100). For high coverage, these consist of groups of sharp O^+ emission spots, whose geometry is a function of adsorption and annealing temperature. O^+ emission normal to the surface was found, as well as off normal spots, whose number and orientation clearly reflect the underlying substrate geometry.

The antibonding state potential funnel is assumed to be the mechanism which produces focussed spot patterns. For a number of the observed ESDIADs, one can discount the possibility that off axis emission is due to thermally activated substrate facetting.[13] Here, only flat substrates are considered.

The peaks in ion energy spectra were found to occur at 8 to 9 ev, on both W(111) and W(100).[6-8] This agrees with earlier studies[5] on polycrystalline tungsten, which report a spectrum peaking at 8.8 ev.

The qualitative features of our result are unaltered by the following choice of models. Spacial variation in the excitation and reneutralization rates was neglected; thus, we chose χ_ϵ and S_2 to be constants. When vibrational states are highly localized, the distortion of σ^+ introduced by this approximation is not critical. Ion energy spectra will be skewed toward lower energies, and the preferential reneutralization of slower ions is neglected.

Near a possible adsorption site, we modelled E_1 as a parabolic potential:

$$E_1(\vec{r}) \simeq -V_0 + \frac{1}{2}(\vec{r}-\vec{b})\overleftrightarrow{K}(\vec{r}-\vec{b})$$

Here, $\vec{b}$ is the adsorption site coordinate. The chemisorption energy V_0 does not appear explicitly in these calculations. The spring constant tensor $\overleftrightarrow{K}$ was taken to be isotropic, for simplicity. One fits $K_{\alpha\beta}$ to the best experimental values.

We chose for P_1^o gaussian distributions both in position and velocity spaces.. This choice is appropriate for particles in an harmonic potential well both for high temperature, and in the zero temperature case. The shape of ion energy spectra results from a folding of P_1^o against E_2 in these calculations. However, peak ion energies are insensitive to the width of P_1^o. The sixfold integration on phase coordinates r_o, v_o in Eqn (10a) was accomplished by the Monte Carlo method.

In modelling E_2, ions were approximated as point charges which respond to the local electrostatic surface potential. The character of the dominent anti-bonding state in ESD is not known: for simplicity, we chose to examine one which leaves the substrate free of excitation. E_2 is taken to be the sum of the unexcited substrate Hartree potential, plus an image contribution, produced by averaged electron density fluctuations, viz:

$$E_2(\vec{r}) \simeq q V_{IM}(\vec{r}) + q \sum_{\vec{R}_j} V_A(\vec{r}-\vec{R}_j)$$

Here, q is the ionic charge. Bonding effects in the substrate were neglected. The surface Hartree potential was represented by the sum of free tungsten atom Hartree potentials centered on the lattice sites. Similar superpositions have been the starting point for self-consistent band structure calculations in bulk tungsten.[14-16]

The Herman-Skillman wave functions[17] were used to evaluate V_A numerically, which was then fitted to the form:

$$V_A(r) \approx 7.72\, e^{-1.29r}$$

All quantities are in atomic units. As a check, we evaluated also the screened tungsten atomic potential in the Fermi-Thomas approximation. At realistic $W\text{-}O^+$ separations, the resulting potential is somewhat smaller than the above.

An ion-surface plasmon hamiltonian[18,19] was used to numerically evaluate the image potential V_{IM}, for a number of values of z and r_s, the plasma parameter. The result for singly ionized atoms was fitted, to the following form:

$$V_{IM}(z, r_s) \approx \frac{-1}{4z + 1.16 + 1.34 r_s + O(r_s^2)}$$

Image charge density resides, in this model, on an approximate electronic boundary of the metal. Including plasmon dispersion shifts the divergence in the classical result at the dielectric surface to the interior of the metal.

Some consequences of this ESD model, on W(111) are now examined. Extensive numerical computation using $100^{\circ}K.$ for the desorption temperature was done, at a wide variety of possible adsorption sites.

The most striking result follows: the naive model constructed for the anti-handling potential strongly focusses ions created in the neighborhood of most plausible candidates for adsorption for sites. The most compact simulated O^+ emission spots are associated with the largest mean ion energies. Long range image attraction tends to defocus the spots. However, this mechanism is competitive with focussing by the repulsive component of E_2 only for very low energy ions.

Each adsorption site candidate produces a single emission spot. For higher energy ions, the local value of $-\vec{\nabla}E_2$ at the point of ionization provides the dominent impulse, and sets both the central colatitude and azimuthal orientation relative to the substrate for the resulting emission spot. In many cases, the dominent contribution to E_2 comes from a single substrate atom. Emission spot geometry then reflects the chemisorption bond direction.

We were successful in generating simulated ion distributions quite similar to those which were observed on W(111). Success, however, in replicating the visual features of ion distributions does not guarantee that this model for the antibonding state is applicable. In particular, the simulated ion energy spectra which were produced peak well below the experimental ion energies. This was the case even for adsorption site candidates whose ESDIAD pattern simulations closely resemble those observed. This finding is discussed further in the concluding section. For now, we remark that remodeling of the anti-bonding state is required.

Despite the limitations of this model, it is useful to explore the most plausible picture of high coverage oxygen chemisorption it can generate, guided by experiment.

Whenever the anti-bonding state potential has the qualitative behavior of our model, the following rules associate the gross features of ESDIAD spot patterns with adsorption geometry. Emission spots directed off the surface normal are evidence of adsorption at a point where E_2 is assymmetric, that is, away from the one fold degenerate unit cell sites. Here, we define n fold degeneracy to mean that a particular point is found in n equivalent locations within a single unit cell whose environments are identical except for combinations of rotation, reflection, and translation. For example, in Fig.(2) all the points labelled 'α','β','γ','δ' are degenerate. At the high symmetry (one fold degenerate) sites, the anti-bonding potential possesses approximate azimuthal symmetry, and thus leads to emission peaked normal to the surface.

One would reconsider this interpretation if long lived, highly localized substrate excitations could be shown to dominate in the anti-bonding potential. Such excitations might be localized on neighboring adsorbate or substrate atoms, and could result in non-normal emission of atoms adsorbed at symmetric points.

Within the model we used, symmetrical groupings of off axis spots are explained. Assymmetric points in the unit cell are several-fold degenerate. An adsorbate domain on the surface in which such sites are occupied should be found, with equal occupation probability, in all degenerate orientations. The corresponding ESDIAD patterns should thus contain spot superpositions suggestive of the substrate unit cell structure.

We illustrate with applications of the model to W (111). Fig. (2) shows the W(111) surface unit cell. Some of the lengths pertinent to the W-O system in are tabulated in Table 1. Here we are guided by experiment. Under conditions for which facetting of the surface is believed not to occur, trios of O^+ emission spots were found, having the substrate orientation shown in Fig. (2) . These were found in conjunction with normal emission, or with a second spot trio, rotated 180^o.

In this simulation, adsorption at the highly assymmetric points such as 'α' or 'β' in fig. (2) can produce only patterns of six spots, rotated from the observed orientation. Adsorption directly over one of the highly symmetric points 'A', 'B', or 'C' produces only emission in a narrow cone normal to the surface. Adsorption elsewhere along the unit cell mirror planes is expected to generate spot trios, with primary oriented spots, as in Fig. (2), corresponding to adsorption between points 'A' and 'C', while 180^o rotated trios correspond to occupied sites between 'C' and 'B', or 'B' and 'A' .

We located those sites which yield the best fit with this anti-bonding potential, to the experimental ESDIAD patterns and ion energies. A reasonable lower limit on the W-O bond length was chosen as 1.95A°, the sum of Slaters atomic radii.[20-22] The colatitude of simulated primary lobes was fitted to the experimental[6] value of 34°.

The most plausible site candidate found for the origin of 'primary' spot trios (i.e., those with the orientation shown in Fig.2) lies almost equidistant from the 'A' and 'C' layer tungsten atoms, in Fig. (2), along the unit cell mirror plane. A site almost equidistant from the 'C' and 'B' layer tungsten atoms is this models best choice for the generator of 180° rotated spot trios.

For both of these sites, the mean energy of emitted ions was calculated to lie in the range 2 to 2.5 ev, which is significantly smaller than the experimental value of 8-9 ev. For the normal emission spot produced by adsorption directly over point 'C', this model predicts ions energies peaking at 1.3 ev. Note that these calculations predict peak ion energies an order of magnitude below experiment, for adsorption sites directly above the surface layer tungsten atoms at 'A'. Fig (3) shows the spot patterns for sites mentioned.

V: DISCUSSION, CONCLUSIONS

The first principles kinetic theory presented above for angular dependence in ESD provides a vehicle for testing model ion-solid interactions. Calculations performed using a simple model for the ground state surface anti-bonding potential predict the strong focussing of ions, like that observed in ESDIAD experiments involving O^+ emission. Models of O^+ chemisorption on W were inferred, by fitting to the experimental patterns. Unfortunately, poor agreement between our calculated ion energy distributions and the experimental[5] ones weakens the plausibility of such chemisorption models, for high oxygen coverage on tungsten. However, we expect these model calculations to apply

to low oxygen coverage on W for which O_2 is believed to dissociate. It is likely at low coverage, that the metallic substrate will support only excitations whose lifetimes are much shorter than ion ejection times.

Complementary model calculations for O^+ desorption from W(100) were done. Some of the results have been reported in the literature.[11] Here, we remark that the ion energy distributions obtained in model computations peak at about 2.5 ev, as for W(111).

Substantially the same picture of adsorption results from a range of models for the antibonding potentials (which are time independent), and which involve basically scale and range changes. More careful modelling of the potential for ground state surfaces may moderately increase the calculated ion energies. For example, we replaced the tungsten wave function by a set which includes L-S coupling,[23] then repeated calculations for some selected sites. Ion energies were increased by a factor of roughly 1.5 to 2, with neglible change in the simulated ESDIAD patterns.

It appears unlikely, however, that a model anti-bonding state in which the substrate and remaining adsorbate atoms are free of excitation can adequately explain the high ion energies observed for β_1 oxygen.

It is interesting to note that ion energy spectra peaking at 1.7 ev. were reported for ESD of H^+ from tungsten.[5] This is consistent with the energy range predicted by our model.

We speculatively suggest that excited antibonding states involving the surface and adsorbate atoms may be able to explain the large O^+ ejection energies found at high coverage. Explicit detailed treatment of these as yet unknown states requires cluster calculations beyond the scope of this work.

The type of processes we suggest are analogous to those involved in electron dissociation of free molecules. A collision with an incident electron

leaves the local surface in a state from which an adsorbate ion dissociates. The local region is left as an excited fragment, which produces the antibonding effective potential governing ion propagation. Excited states may be distributed over an extended cluster, or localized to one or several neighboring atoms.

Surface excitations can produce ion energies in the range observed for O^+ on W, provided their lifetime is long compared to times spent near the surface by ions. Picture a simplistic process, for example, which leaves both O^+ and W^+ on the surface. The coulomb interaction, at 1.95 A^o separation, yields 7-8 ev energies. For O_2 molecules, energies are ~ 12 ev.

In this picture, the lifetimes of surface excitation must be long compared to ionic flight times. Otherwise, the strong anti-bonding potential shuts off immediately after its creation, leaving the ground state surface potential to provide the dominent impulse to desorbing ions, as in the model calculations presented above. Long lifetimes for surface excitations may be justified if one postulates a transition in surface behavior from metallic to insulating, as coverage approaches a full monolayer for oxygen. Note that the experimental O^+ energies pertain to the high coverage β_1 phase.

Insight into the physical reasons for a low yield β_2 and a high yield β_1 oxygen phase can be gained, if this insulating barrier picture is a realistic one for high coverage. In addition to supporting long lived excitations, such a barrier would inhibit ion reneutralization. Both higher ion energies and smaller hopping matrix elements would appear in the reneutralization rate, compared to a low coverage surface. Dramatic increases in the ion survival probability would result, due to the exponential dependence of S_2 on $Q(r)$.

ESD emission of H^+ from W can probably be explained using the ground state surface model, with no need to postulate the formation of an insulating barrier at high coverage. The H^+ yield for both β_1 and β_2 hydrogen phases is small, and comparable to that of oxygen in the low coverage phase.

We can devise speculative mechanisms which produce geometrical spot patterns in ESDIADs, whether it is the ground state surface potential or an excited anti-bonding state which governs ion emission. If the anti-bonding state is associated with highly localized excitations, off axis spots can result even in the case where adsorption occurs at the highly symmetric points of the unit cell. Note, for example, on Fig. (2), that an adsorbate ion created above point 'C', together with excitation of an adjacent 'A' layer tungsten atom, can produce downward facing spot trios. If excited states are multi-centered, the anti-bonding potential will have essentially the same symmetry as the ground state potential. Off axis spot groups then correspond to adsorption at points in the unit cell away from the symmetry sites.

The speculative nature of some of our remarks indicates the need for accelerated theoretical study of ESD mechanisms, after which unambiguous adsorption site determinations using ESDIAD may be made.

REFERENCES

1. Gomer, R., Sol. St. Phys. 30, 94-226 (1975).
2. Menzel, D., Surface Science 47, 370 (1975).
3. Madey, T. E., J. T. Yates Jr., J. Vac. Sci. Tech. 8, 525 (1971).
4. Leck, J. H., B. P. Stimpson, J. Vac. Sci. Tech. 9, 273 (1972).
5. Nishijima, M., F. M. Propst, Phys. Rev. B2, 2368 (1970).
6. Madey, T. E., J. Czyzewski, J. T. Yates, Jr., Surf. Sci. 57, 580 (1976).
7. Czyzewski, J., T. E. Madey, J. T. Yates, Jr., Phys. Rev. Lett. 32, 777 (1974).
8. Madey, T. E., J. Czyzewski, J. T. Yates Jr., Surf. Sci. 49, 465 (1975).
9. Menzel, D., R. Gomer, J. Chem. Phys. 41, 3311, 3329 (1964).
10. Redhead, P. A., Can. J. Phys. 42, 886 (1964).
11. Gersten, J., R. Janow, N. Tzoar, Phys. Rev. Lett. 36, 610 (1976).
12. Gersten, J., R. Janow, N. Tzoar, Phys Rev. B11, 1267 (1975).
13. Tracy, J. C., J. M. Blakely, Surf. Sci. 13, 313 (1968).
14. Dimmock, J. O., Sol. St. Phys. 26, 103-274 (1971).
15. Matheiss, L. F., Phys. Rev. 139, A1893 (1965).
16. Loucks, T. L., Phys. Rev. 143, 506 (1966).
17. Herman, F., S. Skillman, Atomic Structure Calculations, Prentice Hall (1965).
18. Tzoar, N., J. Gersten, Phys. Rev. B8, 5671,5684 (1973).
19. Gersten, J., N. Tzoar, Phys. Rev. B9, 4038 (1974).
20. Slater, J. C., Quantum Theory of Molecules and Solids, Vol. II, Mc-Graw Hill (1965).
21. Pauling, L., The Nature of the Chemical Bond, 3rd Ed., Cornell Univ. (1960).
22. Van Hove, M., S. Tong, Phys Rev Lett. 36, 1092 (1975).
23. Liberman, D., J. Waber, D. Cromer, Phys. Rev. 137, A27 (1965).

FIGURE CAPTIONS

Fig. 1 The one dimensional qualitative behavior of effective potentials for ionic ESD, as functions of z coordinate. V_o is the chemisorption energy. The z coordinate of the adsorption site is 'b'. The The metal + adsorbate system in its ground state, designated by (M + A), has the potential function $E_1(r)$. An anti-bonding potential $E_2(r)$ leading to ionic ESD is denoted $(M + A^+)$. The substrate here is free of excitation. The dashed line $(M^* + A^+)$ suggests the behavior of the effective potential for an ion interacting with the excited substrate. The asymptotic energy difference $E_2 - E_1$ is V_I, the atomic ionization potential, if both incident and ejected electrons are Auger emitted to the vacuum.

Fig. 2 The W(111) surface unit cell. Large spheres depict tungsten atoms. The 'A' atoms lie in the surface layer. 'B' and 'C' atoms reside in the second and third planes in the solid. The A-A distance is 8.44 a_o. Dashed lines through "B', 'C' are bilateral symmetry axes. 'Primary' ESD emission lobes for O^+ on W(111) have been observed, with their substrate registry as indicated by the trio of heavy circles.

Fig. 3 Simulated ESD spot patterns for low coverage of Oxygen on W(111). Fig. 3a shows the ion distributions for adsorption 1.95 A^o. over point 'C' on Fig. 2. Fig. 3b corresponds to adsorption almost equidistant from tungsten atoms at 'A' and 'C', while Fig. 3c pertains to adsorption between sites 'C' and 'B'. This series provides the best fit to experimental patterns of Madey, et al.

Empirical Atomic Radii:

Oxygen	(Slater)	0.60 A.°
	(Pauling)	0.66
Tungsten	(Slater)	1.35
	(Pauling)	1.30

Bulk Tungsten (B. C. C.) Lengths:

Lattice Constant	3.16
W - W interatomic spacing	2.74

W(111) Surface Lengths:

Lattice Constant	4.47
Interplanar spacing	0.91

W(100) Surface Lengths:

Lattice Constant	3.16
Interplanar spacing	1.58

W - O Bond Lengths:

Sum of Empirical Atomic Radii	(Slater)	1.95
	(Pauling)	1.96
Experimental W-O bond Length on W(110) (ref.22)		2.08 $\pm$ .07 A°.

TABLE 1: Some Characteristic Lengths in the Tungsten- Oxygen System. Unless noted otherwise, lengths are taken from either Ref. 20 or 21.

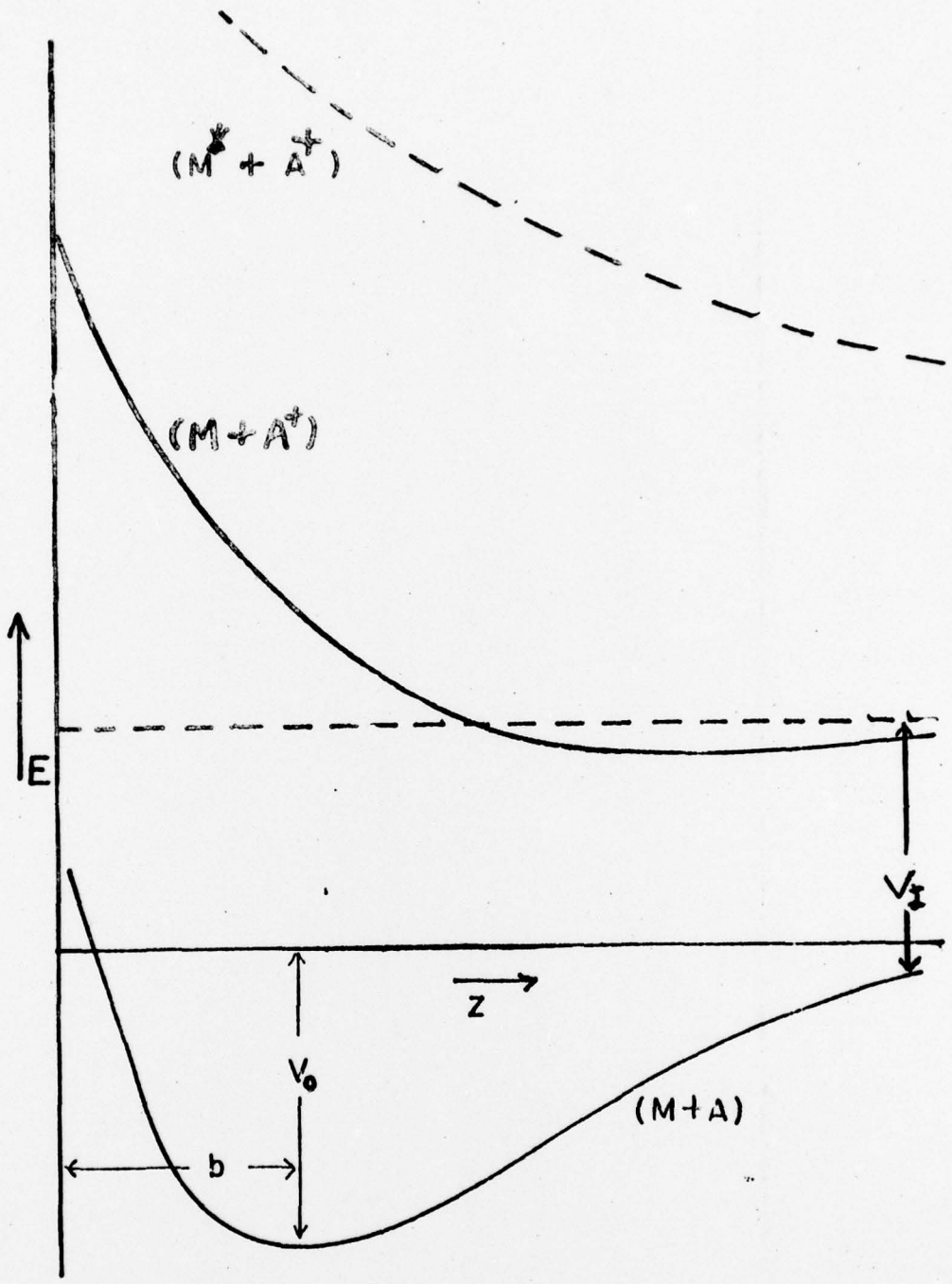

FIG. 1

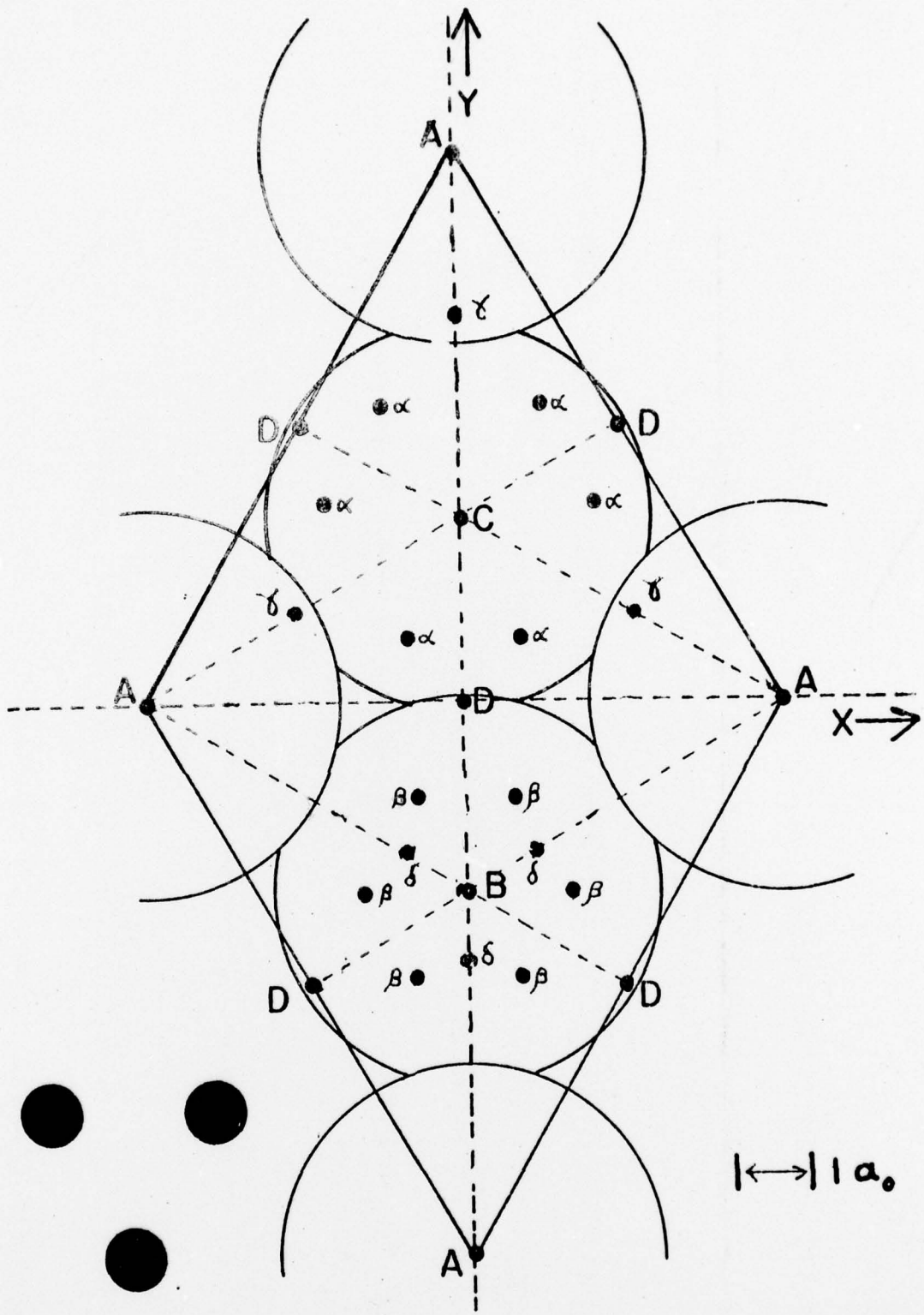

FIGURE 2

M1016
23-Jul-76

X = TAN(THETA) COS(PI
Y = TAN(THETA) SIN(PI

SIMULATED ESD PATTERN 3

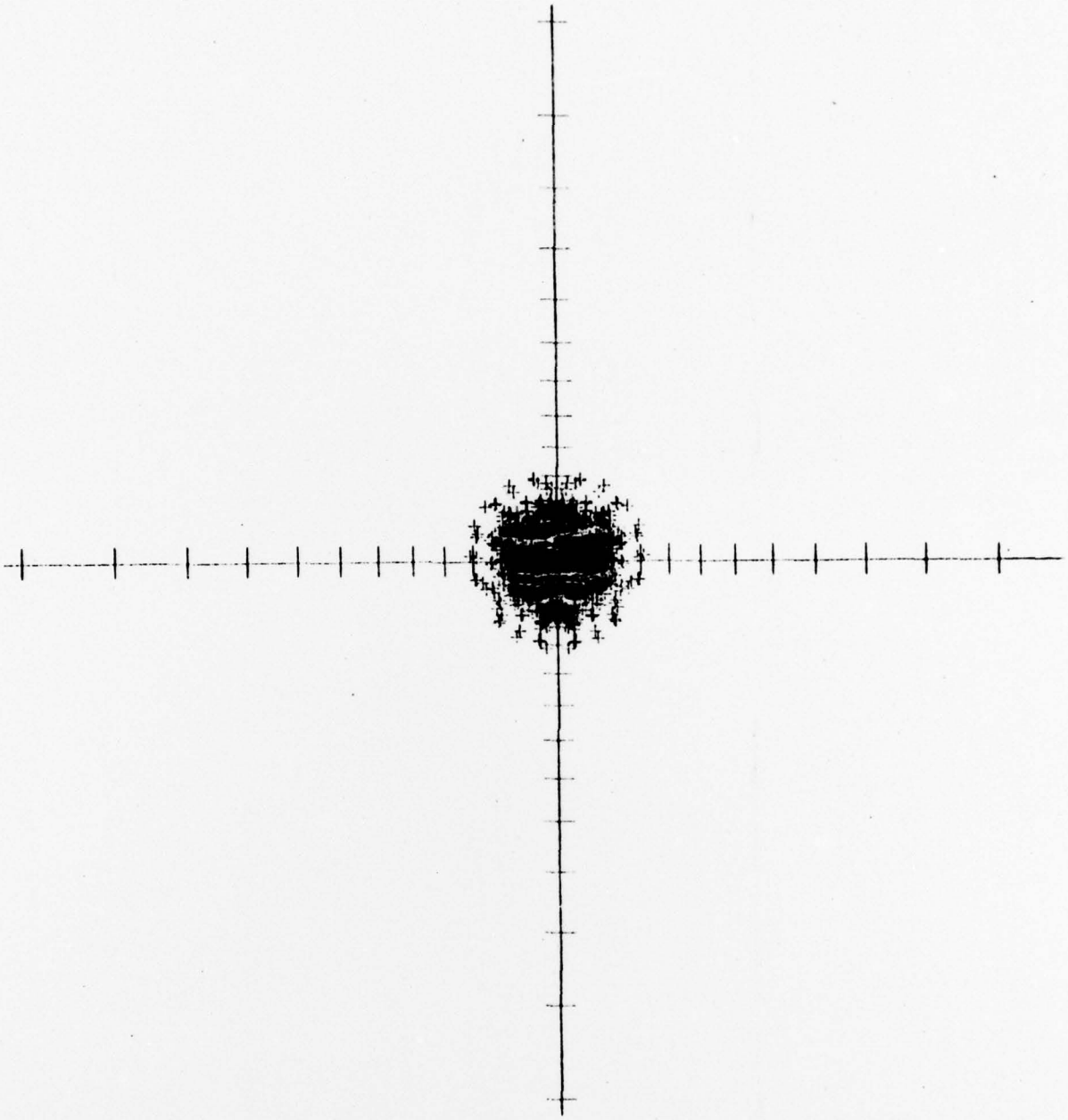

SCALE FACTOR .280
5 DEGREE SCALE

3000 POINTS PLOTTE
0 POINTS OFF S

FIGURE 3a

X = TAN(THETA)COS(PHI)
Y = TAN(THETA)SIN(PHI)

SIMULATED ESD PATTERN 3

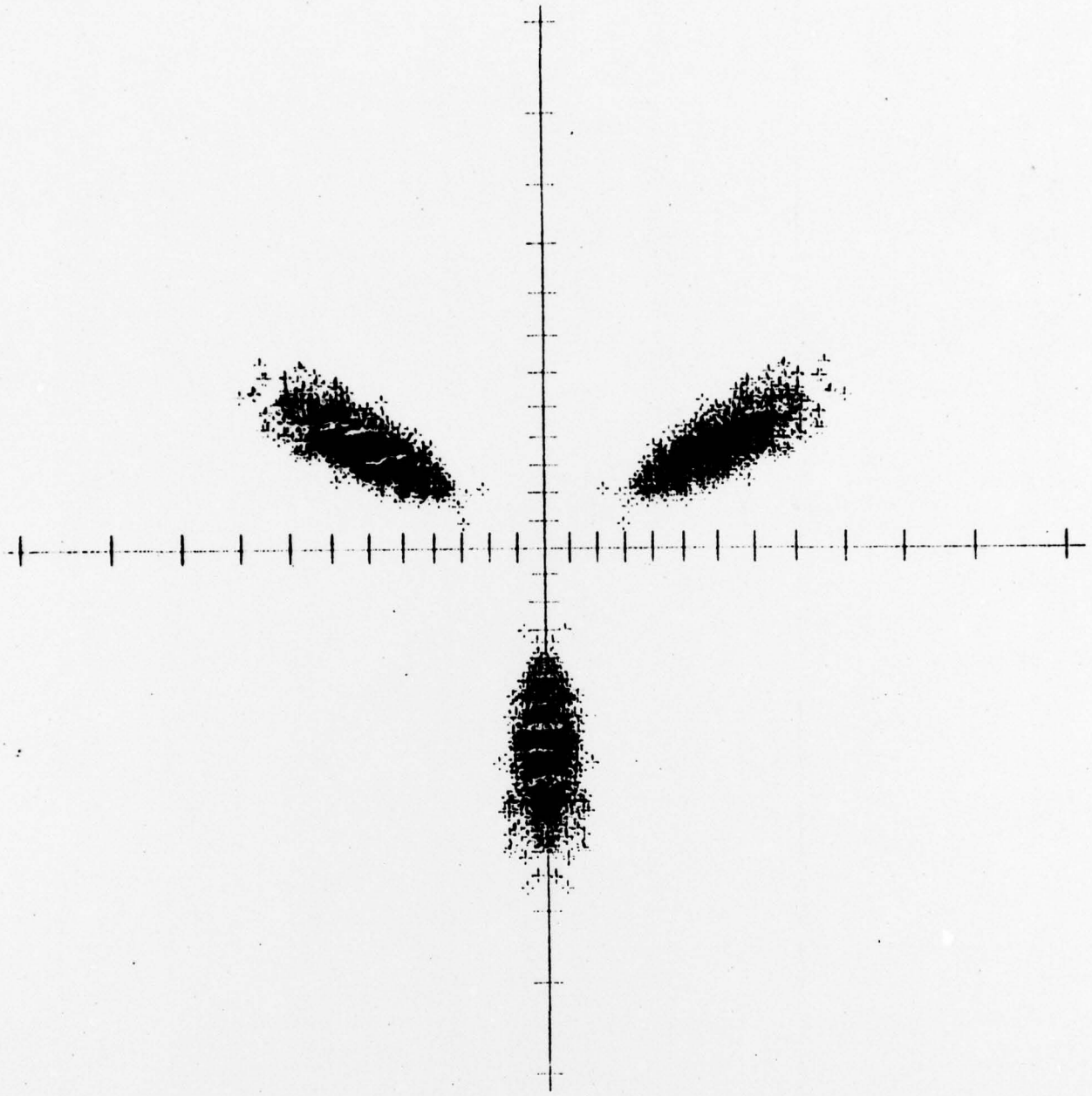

SCALE FACTOR .750
SET FOR SCALE

5000 POINTS PLOTTED
0 POINTS OFF SCALE

FIGURE 3b

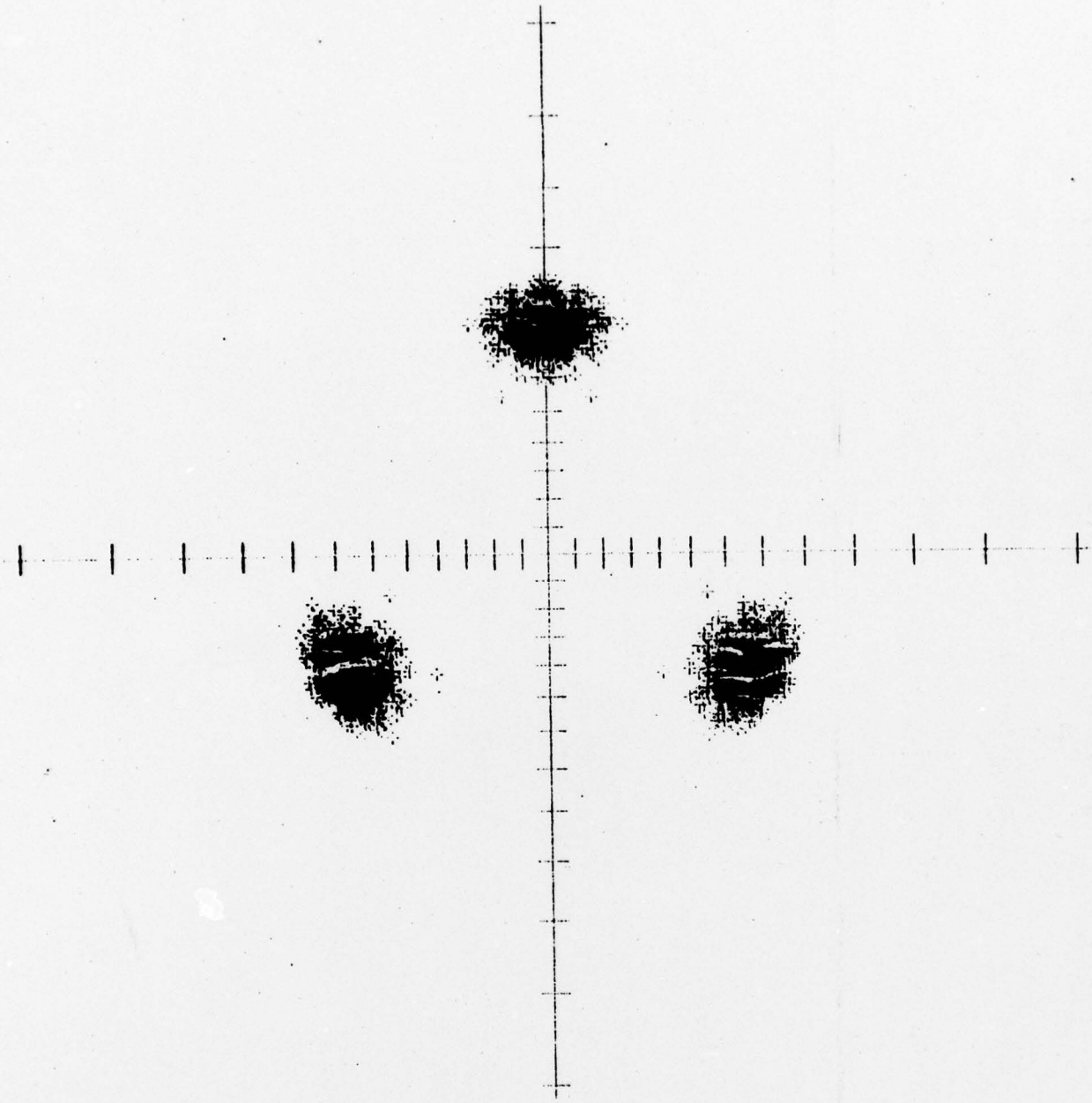

FIGURE 3c